Electronic Supplementary Material (ESI) for Chemical Communications
This journal is © The Royal Society of Chemistry 2013

Supplementary Information

for

# The evolution of spin distribution in the photoexcited triplet state of ethyne-elaborated porphyrins

Paul J. Angiolillo*, Jeff Rawson, Paul R. Frail, and Michael J. Therien*

**Instrumentation.** Electronic absorption spectra were recorded on an OLIS UV/vis/NIR spectrophotometry system that is based on the optics of a Cary 14 spectrophotometer. Steady-state emission spectra were recorded on a SPEX Fluorolog-3 system equipped with a red sensitive Hamamatsu R2638 PMT or a liquid nitrogen cooled InGaAs detector. Electron paramagnetic spectroscopy experiments were performed with a Bruker ESP 300E spectrometer and on Varian E-109 spectrometer. Optical pumping of the triplet manifold was accomplished through intracavity excitation through a fiber optic cable. The excitation source was a 150 W quartz-halogen illuminator from Kuda, Mitsubishi Corporation. Appropriate filtration of infrared radiation was accomplished using a Corning blue heat filter. Temperatures were maintained utilizing an Oxford ESR 900 continuous flow liquid helium cryostat regulated with an Oxford ITC4 temperature controller. Temperatures reported are within ±1 K using this system over the temperature ranges studied. Microwave frequency was determined using a Hewlett-Packard 5350B frequency counter, which can be traced to the National Institutes of Standards and Technology. All experiments were conducted at microwave powers (2-10 μW) that ensured resonance saturation did not occur. EPR spectra of the optically pumped triplet states were obtained through numerical subtraction of spectra obtained without irradiation

from those obtained during irradiation. Optical absorption spectra of all compounds were obtained after EPR spectral collection in order to monitor any photodegradation processes. No evidence of photodegradation was observed.

**Computational Methods.** Initial structures were generated using the Spartan Student package.[1] Two truncations were made in the interest of computational economy; aryl groups were abbreviated as phenyl, and all silyl groups were replaced with trimethylsilyl groups. Figures S-6 through S-13 include depictions of the structures used for these calculations.

Structure optimizations and time-dependent SCF calculations were performed with Density Functional Theory (DFT) using Gaussian 09, Rev C.1.[2] The Becke three-parameter hybrid[3] and the Lee-Yang-Parr correlation functional[4] were employed for all calculations (B3LYP). Final optimizations were performed to tight convergence criteria (keyword 'SCF=tight'); initial optimizations used smaller basis sets but the final optimized structures were all produced using the 6-311g basis set,[5] with each nonhydrogen atom given one set of diffuse functions and one set of d polarization functions (6-311+G(d)) as implemented in Gaussian 09. TDDFT calculations were performed on the optimized structures using this same basis set; no solvation model was employed. B and Q transitions were assigned based upon comparison of the computed energies to the experimental spectra; x- and y-polarized transitions were assigned by analogy of the involved configurations to established literature.[6]

**Materials.** All manipulations were carried out under nitrogen or argon previously passed through an $O_2$ scrubbing tower (Schweizerhall R3-11 catalyst) and a drying tower (Linde 3-Å molecular sieves) unless otherwise stated. Air-sensitive solids were handled in a Braun 150-M glove box. Standard Schlenk techniques were employed to manipulate air-sensitive solutions. All solvents utilized in this work were obtained from Fisher Scientific (HPLC Grade). Tetrahydrofuran (THF) was distilled from Na/benzophenone under $N_2$. Diethylamine and triethylamine were dried over KOH pellets and distilled under vacuum. All NMR solvents were used as received. TBAF 1M in THF, trimethylsilylacetylene, triisopropylsilylacetlyene, triethylsilylacetylene, 1,4-bis-trimethylsilylbutadiyne, $Pd_2dba_3$, $AsPh_3$, $Pd[(PPh)_3]_4$ and copper(I)iodide were used as received (Aldrich or GFS Chemicals). 2,2'-Dipyrrylmethane,[7] 1-bromo-2-(triethylsilyl)ethyne and 1-bromo-2-(triisopropylsilyl)ethyne,[8] 3-triisopropylsilyl-propynal, 5,10,15,20-tetrakis(triisopropylsilylethynyl)porphyrin, 5,10,15,20-tetrakis(triisopropylsilylethynyl)porphinato)zinc(II)[9] (**PZn-cross**) were prepared according to literature procedures. 1,3-bis(3,3-dimethylbutoxy)benzene, 2,6-bis(3,3-dimethylbutoxy)benzaldehyde, 5,15-bis(2',6'-bis(3,3-dimethylbutoxy)phenyl-porphyrin, 5-bromo-10,20-bis(2',6'-bis(3,3-dimethylbutoxy)phenyl-porphyrin, 5,15-dibromo-10,20-bis(2',6'-bis(3,3-dimethylbutoxy)phenyl-porphyrin, [5-bromo-10,20-bis(2',6'-bis(3,3-dimethylbutoxy)phenyl-porphinato]zinc(II) and [5,15-dibromo-10,20-bis(2',6'-bis(3,3-dimethylbutoxy)phenyl-porphinato]zinc(II), [5-triisopropylsilylethynyl-10,20-bis(2',6'-bis(3,3-dimethylbutoxy)phenyl-porphinato]zinc(II) (**PZn-E**), [5,15-bis(triisopropylsilylethynyl)-10,20-bis(2',6'-bis(3,3-dimethylbutoxy)phenyl-porphinato]zinc(II) (**E-PZn-E**), [5-ethynyl-10,20-bis(2',6'-bis(3,3-

dimethylbutoxy)phenyl-porphinato]zinc(II), and [5,15-diethynyl-10,20-bis(2',6'-bis(3,3-dimethylbutoxy)phenyl-porphinato]zinc(II) were prepared by established methods.[10] Chemical shifts for $^1$H-NMR spectra are relative to solvent residual protium ($CDCl_3$, δ = 7.24 ppm; pyridine-$d_5$, δ = 8.71 ppm; THF-$d_8$, δ = 3.58 ppm). All *J* values are reported in Hertz. The number of attached protons is found in parentheses following the chemical shift value. Chromatographic purification (silica gel 60, 230-400 mesh, EM Scientific) of all compounds was accomplished on the bench top. High resolution mass spectroscopic analyses were performed at the University of Pennsylvania Mass Spectrometry Center.

**[5-Trimethylsilylbutadiynyl-10,20-di(2',6'-bis(3,3-dimethylbutoxy)phenyl)porphinato]zinc(II) (PZn-EE).** [5-Bromo-10,20-di(2',6'-bis(3,3-dimethylbutoxy)phenylporphinato]zinc(II) (804 mg, 0.80 mmol), $Pd(PPh_3)_4$ (92 mg, 0.08 mmol), and THF (30 mL) were brought together in an oven-dried 100 mL Schlenk tube and deaerated via three freeze-pump-thaw cycles. 1,4-Bis-trimethylsilylbutadiyne (1.56 g, 8.0 mmol) was placed in a 50 mL Schlenk tube and diluted with THF (10 mL) and cooled to 0° C with stirring. Methyl lithium–lithium bromide (5.1 mL, 1.5 M) was added dropwise to the 1,4-bis-trimethylsilylbutadiyne solution and brought to room temperature. The solution was transferred via cannula to a 250 mL Schlenk flask containing $ZnCl_2$ (1.64 g, 12.0 mmol) in 30 mL of THF. The resulting trimethylsilylbutadiynyl-zinc chloride solution was stirred at room temperature for about 30 minutes and the porphyrin solution was transferred to the 250 mL flask and stirred at 60° C for 20 h. The reaction was cooled and the solvent was evaporated. The residue was redissolved in a minimal amount of THF adsorbed to silica (100 g). The

product was purified by chromatography using THF:hexanes (20:80) as the eluant. The product was collected as a greenish purple band and evaporated to give 780 mg of the desired porphyrin (93% based on the [5-bromo-10,20-di(2',6'-bis(3,3-dimethylbutoxy)phenylporphinato]zinc(II) starting material). $^1$H NMR (250 MHz, $CDCl_3$:pyridine-$d_5$ 20:1): 9.89 (s, 1 H), 9.50 (d, 2 H, $J$ = 4.6 Hz), 9.09 (d, 2 H, $J$ = 4.5 Hz), 8.83 (d, 2 H, $J$ = 4.6 Hz), 8.79 (d, 2 H, $J$ = 4.4 Hz), 7.68 (t, 2 H, $J$ = 8.4 Hz), 6.98 (d, 4 H, $J$ = 8.4 Hz), 3.87 (t, 8H, $J$ = 7.5 Hz), 0.74 (t, 8 H, $J$ = 7.6 Hz), 0.32 (s, 36 H), 0.16 (s, 9 H). MS (MALDI-TOF) *m/z*: 1044.5 (calcd for $C_{63}H_{76}N_4O_4SiZn$ ($M^+$) 1044.5).

**[5-Triethylsilylhexatriynyl-10,20-di(2',6'-bis(3,3-dimethylbutoxy)phenyl)porphinato]zinc(II) (PZn-EEE)**. Compound **16** (390 mg, 0.4 mmol), hydroxylamine hydrochloride (500 mg, 7.2 mmol), copper(I)chloride (500 mg, 5 mmol), ethylamine (8 mL, 2M in THF), and DMF (10 mL) were brought together in a 50 mL flask with stirring. 1-Bromo-2-(triethylsilyl)ethyne (800 mg, 3.6 mmol) was added dropwise and stirred for 2 h. The reaction mixture was poured into water and extracted with chloroform (3 x 100 mL). After removal of volatiles, the residue was purified by column chromatography using THF:hexanes (15:85) as the eluant. The product was collected as a dark green band, giving 276 mg of product (62% yield, based on 390 mg of compound **16**. $^1$H NMR (250 MHz, $CDCl_3$:pyridine-$d_5$ 20:1): 9.86 (s, 1 H), 9.42 (d, 2 H, $J$ = 4.5 Hz), 9.06 (d, 2 H, $J$ = 4.4 Hz), 8.82 (d, 2 H, $J$ = 4.7 Hz), 8.76 (d, 2 H, $J$ = 4.4 Hz), 7.66 (t, 2 H, $J$ = 8.3 Hz), 6.97 (d, 4 H, $J$ = 8.4 Hz), 3.85 (t, 8 H, $J$ = 7.6 Hz), 1.02 (t, 9 H, $J$ = 7.9 Hz), 0.73 (t, 8 H, $J$ = 7.5 Hz), 0.68 (q, 6 H, $J$ = 7.9 Hz), 0.30 (s, 36 Hz). MS (MALDI-TOF) *m/z*: 1108.0 (calcd for $C_{68}H_{82}N_4O_4SiZn$ ($M^+$) 1110.5).

**[5,15-Bis-trimethylsilylbutadiynyl-10,20-di(2',6'-bis(3,3-dimethylbutoxy)phenyl)porphinato]zinc(II) (EE-PZn-EE).** [5,15-Dibromo-10,20-di(2',6'-bis(3,3-dimethylbutoxy)phenylporphinato]zinc(II) (868 mg, 0.80 mmol), $Pd(PPh_3)_4$ (92 mg, 0.08 mmol), and THF (30 mL) were brought together in an oven-dried 100 mL Schlenk tube and deaerated via three freeze-pump-thaw cycles. 1,4-Bis-trimethylsilylbutadiyne (1.56 g, 8.0 mmol) was placed in a 50 mL Schlenk tube and diluted with THF (10 mL) and cooled to 0° C with stirring. Methyl lithium–lithium bromide (5.1 mL, 1.5 M) was added dropwise to the 1,4-bis-trimethylsilylbutadiyne solution and brought to room temperature. The solution was transferred via cannula to a 250 mL Schlenk flask containing $ZnCl_2$ (1.64 g, 12.0 mmol) in 30 mL of THF. The resulting trimethylsilylbutadiynyl-zinc chloride solution was stirred at room temperature for about 30 minutes and the porphyrin solution was transferred to the 250 mL flask and stirred at 60° C for 20 h. The reaction was cooled and the solvent was evaporated. The residue was redissolved in a minimal amount of THF adsorbed to silica (100 g). The product was purified by chromatography using THF:hexanes (12:88) as the eluant. The product was collected as a green band and evaporated to give 1050 mg of the desired porphyrin (90% based on the [5,15-dibromo-10,20-di(2',6'-bis(3,3-dimethylbutoxy)phenylporphinato]zinc(II) starting material). $^1$H NMR (250 MHz, $CDCl_3$:pyridine-$d_5$ 20:1): 9.42 (d, 4 H, $J$ = 4.6 Hz), 8.71 (d, 4 H, $J$ = 4.6 Hz), 7.67 (t, 2 H, $J$ = 8.3 Hz), 6.98 (d, 4 H, $J$ = 8.4 Hz), 3.86 (t, 8H, $J$ = 7.5 Hz), 0.75 (t, 8 H, $J$ = 7.5 Hz), 0.34 (s, 18 H), 0.33 (s, 36 H). MS (MALDI-TOF) *m/z*: 1164.5 (calcd for $C_{70}H_{84}N_4O_4Si_2Zn$ ($M^+$) 1165.8).

**[5,15-Bis-triethylsilylhexatriynyl-10,20-di(2',6'-bis(3,3-dimethylbutoxy)phenyl)porphinato]zinc(II) (EEE-PZn-EEE)**. Compound **17** (307 mg, 0.30 mmol), hydroxylamine hydrochloride (500 mg, 7.2 mmol), copper(I)chloride (500 mg, 5 mmol), ethylamine (8 mL, 2M in THF), and DMF (10 mL) were brought together in a 50 mL flask with stirring. 1-Bromo-2-(triethylsilyl)ethyne (800 mg, 3.6 mmol) was added dropwise and stirred for 2 h. The reaction mixture was poured into water and extracted with chloroform (3 x 100 mL). After removal of volatiles, the residue was purified by column chromatography using THF:hexanes (15:85) as the eluent. The product was collected as a dark green band, giving 210 mg of product (54% yield, based on 307 mg of compound **17**. $^1$H NMR (250 MHz, $CDCl_3$:pyridine-$d_5$ 20:1): 9.35 (d, 4 H, $J$ = 4.8 Hz), 8.71 (d, 4 H, $J$ = 4.6 Hz), 7.67 (t, 2 H, $J$ = 8.3 Hz), 6.96 (d, 4 H, $J$ = 8.5 Hz), 3.86 (t, 8 H, $J$ = 7.6 Hz), 1.03 (t, 18 H, $J$ = 7.9 Hz), 0.76 (t, 8 H, $J$ = 7.6 Hz), 0.68 (q, 12 H, $J$ = 7.9 Hz), 0.32 (s, 36 H). MS (MALDI-TOF) *m/z*: 1298 (calcd for $C_{80}H_{96}N_4O_4Si_2Zn$ ($M^+$) 1296.6).

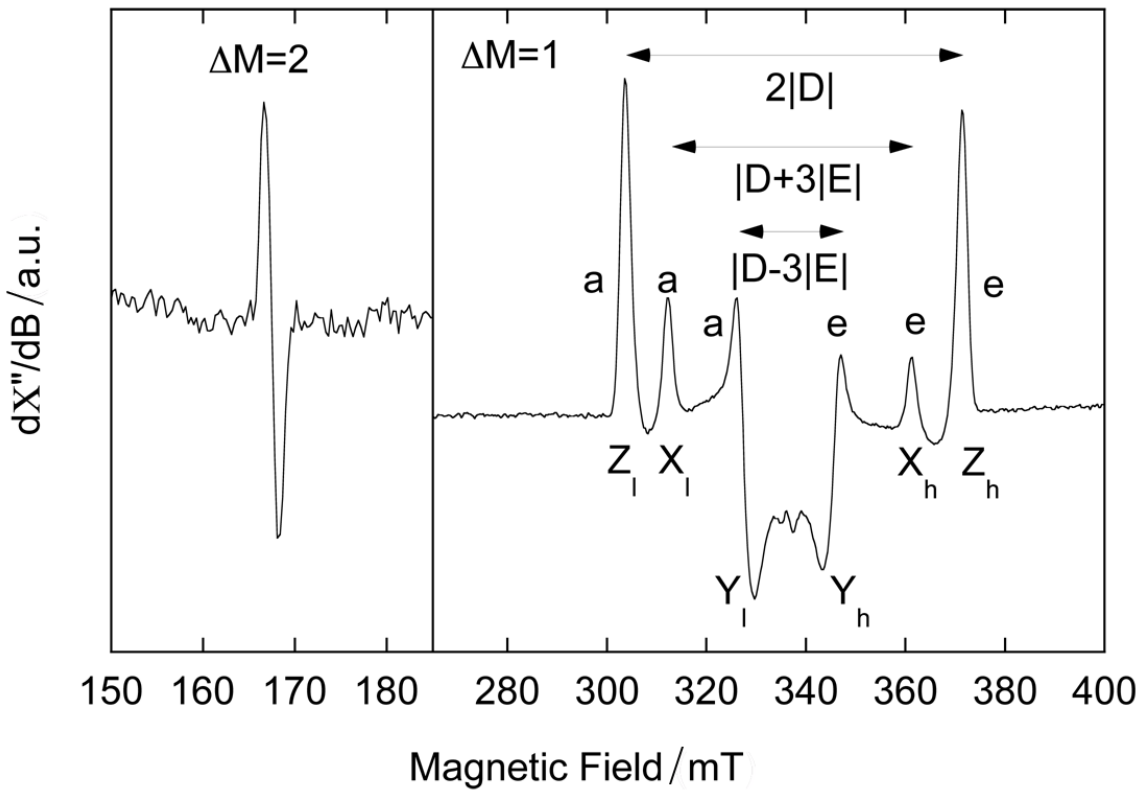


**Fig. S1** Anatomy of the photoexcited triplet state EPR spectrum. EPR spectrum of approximately 500 μM PZn at 4 K in 10% pyr/tol glass under CW irradiation. EPR parameters: temperature, 4K; microwave power, 2μW; modulation amplitude 1 mT at 100 kHz. Absorptive and emissive resonances have been labeled a and e, respectively. The |DM|=2 transition is a forbidden transition from |-1> to the |+1> high-field spin states and is diagnostic of an S=1 spin state.

**Table S1.** Visible Optical Transition Data and ZFS Parameters for Benchmark PZn monomers and ethynyl-elaborated monomers. |D| and |E| ZFS vales are $\pm 0.0002$ cm$^{-1}$.

| | $Q_{(1,0)}$ (cm$^{-1}$) | $Q_{(1,0)}$ (eV) | log ε $Q_{(1,0)}$ | $Q_{(0,0)}$ (cm$^{-1}$) | $Q_{(0,0)}$ (eV) | log ε $Q_{(0,0)}$ | log ε($Q_{(0,0)}$)/ log ε($Q_{(1,0)}$) | \|D\| (cm$^{-1}$) | \|D\| (Hz) | \|E\| (cm$^{-1}$) | \|E\| (Hz) | 3\|E\|/\|D\| | Ref. |
|---|---|---|---|---|---|---|---|---|---|---|---|---|---|
| PZn | | | | | | | | 0.0360 | 1.08 X $10^{+9}$ | 0.0092 | 2.76 X $10^{+8}$ | 0.767 | [11] |
| ZnTPP | 18019 | 2.234 | 4.23 | 16835 | 2.087 | 3.76 | 0.889 | 0.0306 | 9.17 X $10^{+8}$ | 0.0095 | 2.85 X $10^{+8}$ | 0.931 | [12] |
| PZn-cross | 16393 | 2.032 | 4.33 | 15198 | 1.884 | 4.69 | 1.083 | 0.0285 | 8.54 X $10^{+8}$ | 0.0076 | 2.28 X $10^{+8}$ | 0.802 | This work |
| | | | | | | | | | | | | | |
| | $Q_{(1,0)}$ (cm$^{-1}$) | $Q_{(1,0)}$ (eV) | log ε $Q_{(1,0)}$ | $Q_{(0,0)}$ (cm$^{-1}$) | $Q_{(0,0)}$ (eV) | log ε $Q_{(0,0)}$ | log ε($Q_{(0,0)}$)/ log ε($Q_{(1,0)}$) | \|D\| (cm$^{-1}$) | \|D\| (Hz) | \|E\| (cm$^{-1}$) | \|E\| (Hz) | 3\|E\|/\|D\| | |
| ZnDPP | 18430 | 2.285 | 4.03 | 17256 | 2.140 | 3.21 | 0.797 | 0.0326 | 9.77 X $10^{+8}$ | 0.0094 | 2.82 X $10^{+8}$ | 0.865 | [12] |
| PZnE | 17762 | 2.202 | 4.23 | 16502 | 2.046 | 4.02 | 0.950 | 0.0315 | 9.44 X $10^{+8}$ | 0.0048 | 1.44 X $10^{+8}$ | 0.457 | [12] |
| EPZnE | 17513 | 2.171 | 4.07 | 15773 | 1.956 | 4.47 | 1.098 | 0.0301 | 9.02 X $10^{+8}$ | 0.0053 | 1.59 X $10^{+8}$ | 0.528 | [12] |
| PZnEE | 17668 | 2.191 | 4.2 | 16287 | 2.019 | 4.33 | 1.031 | 0.0334 | 1.00 X $10^{+9}$ | 0.0073 | 2.19 X $10^{+8}$ | 0.656 | This work |
| PZnEEE | 17483 | 2.168 | 4.15 | 16051 | 1.990 | 4.54 | 1.094 | 0.0355 | 1.06 X $10^{+9}$ | 0.0084 | 2.52 X $10^{+8}$ | 0.710 | This work |
| PZn-cross | 16393 | 2.032 | 4.33 | 15198 | 1.884 | 4.69 | 1.083 | 0.0285 | 8.54 X $10^{+8}$ | 0.0076 | 2.28 X $10^{+8}$ | 0.802 | This work |
| EEPZnEE | 16722 | 2.073 | 3.96 | 15291 | 1.896 | 4.71 | 1.189 | 0.0309 | 9.26 X $10^{+8}$ | 0.0084 | 2.52 X $10^{+8}$ | 0.816 | [12] |
| EEEPZnEEE | 16260 | 2.016 | 3.9 | 14749 | 1.829 | 5.05 | 1.295 | 0.0336 | 1.01 X $10^{+9}$ | 0.011 | 3.30 X $10^{+8}$ | 0.982 | This work |

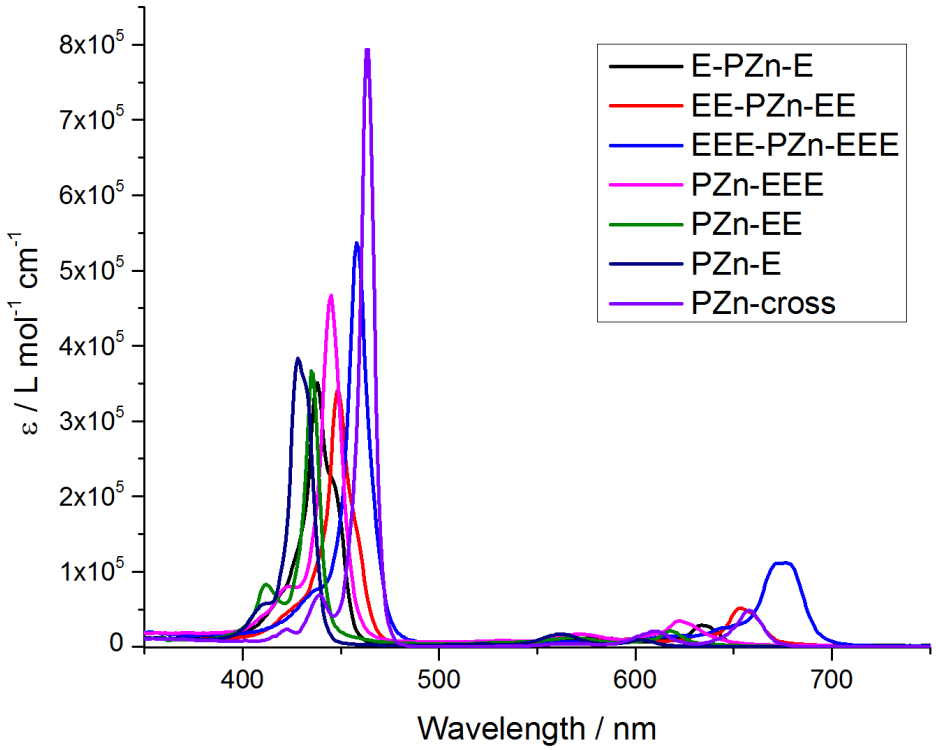


**Fig. S2** Overlay of the electronic absorption spectra of representative ethynyl-elaborated PZn complexes recorded in THF solvent at 298 K.

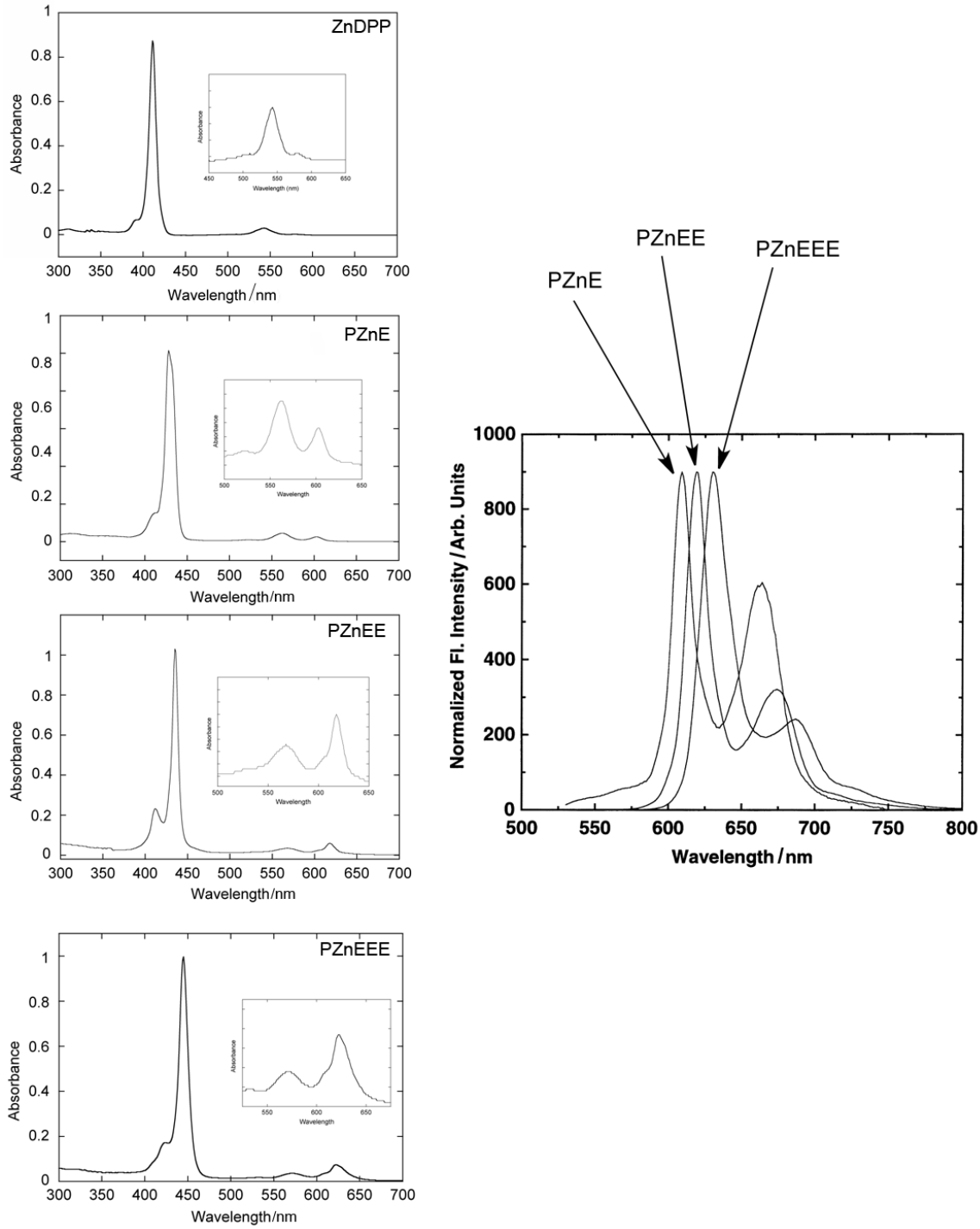


**Fig. S3** Electronic absorption spectra (left) and normalized emission spectra (right) of ZnDPP, PZnE, PZnEE, and PZnEEE recorded in THF solvent at 298 K.

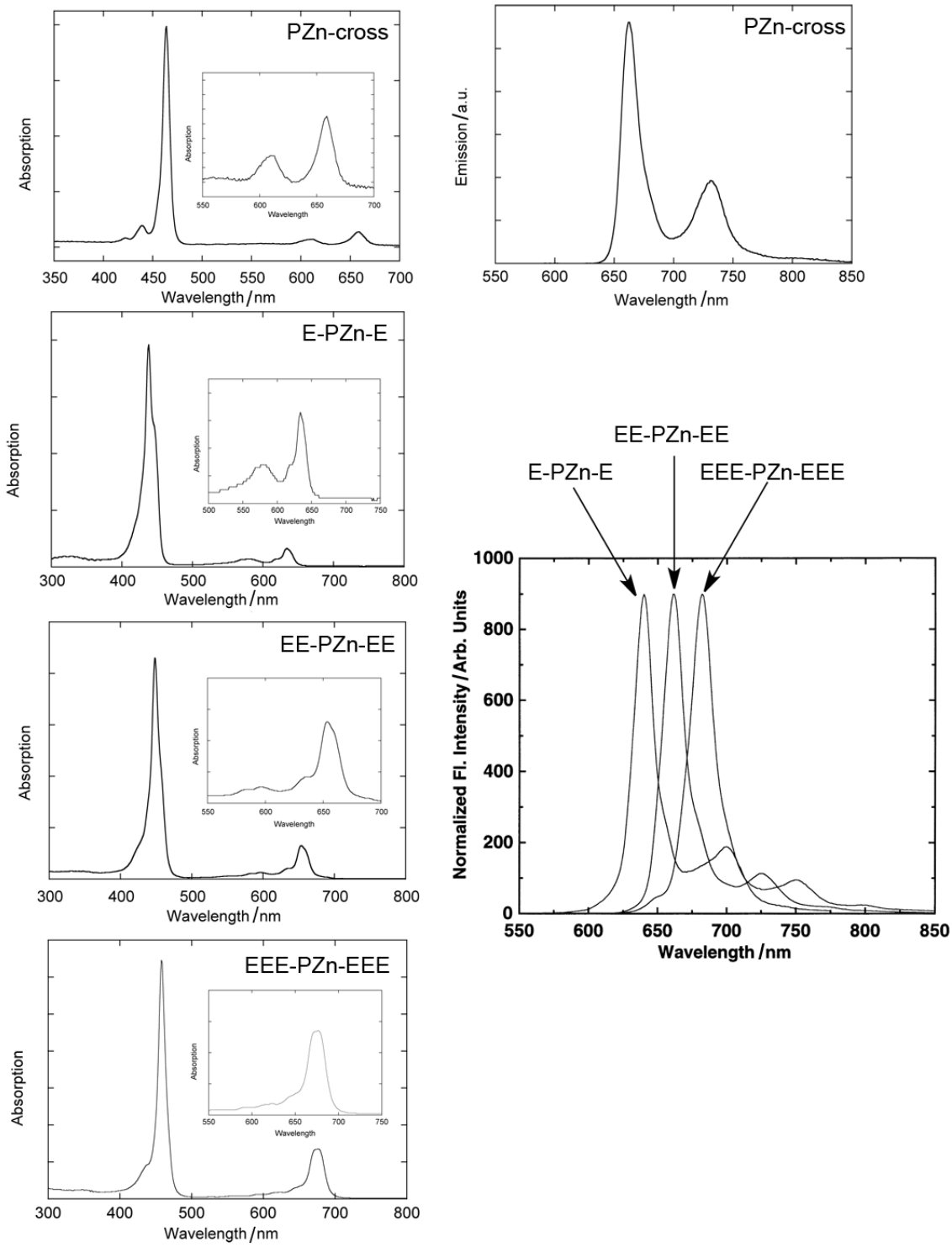


**Fig. S4** Electronic absorption spectra (left) and normalized fluorescence emission spectra (right) of PZn-cross, EPZnE, EEPZnEE, and EEEPZnEEE recorded in THF solvent at 298 K.

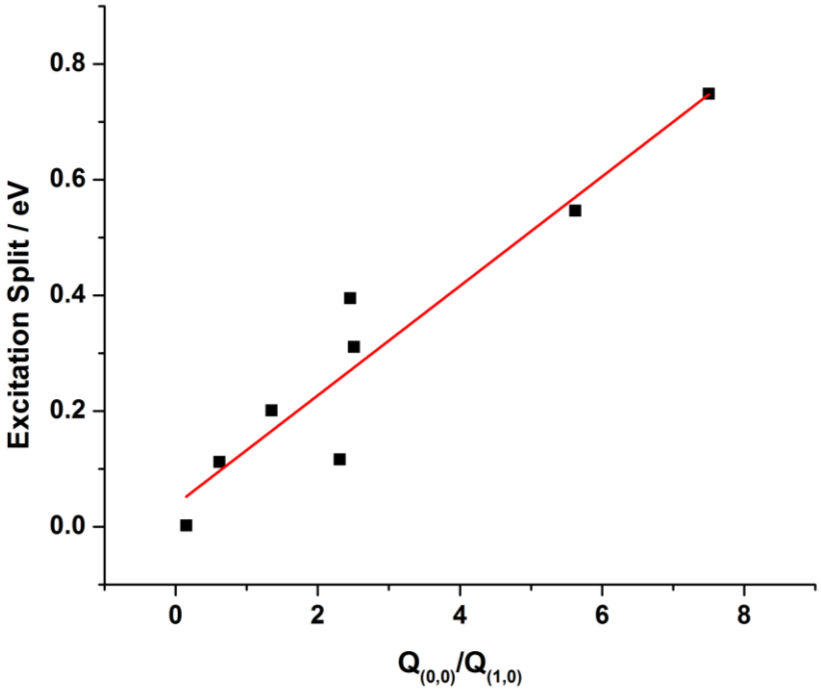


**Fig. S5** Plot of the ratio of the [0,0] to [1,0] absorption intensities versus the energetic difference between HOMO and HOMO-1 originated $Q_X$ configurations.

**Table S2** Experimentally determined oscillator strengths and TDDFT-calculated percentage contributions of individual configurations to the Q transitions of ethyne-elaborated PZn.

| porphyrin | Measured oscillator strengths | | Calculated configuration contribution to $Q_X$ | | Calculated configuration contribution to $Q_Y$ | |
|---|---|---|---|---|---|---|
| | B[a] | Q[b] | HOMO-1 →LUMO+1 | HOMO →LUMO | HOMO-1 →LUMO | HOMO →LUMO+1 |
| ZnDPP | 0.6477 | 0.03192 | 47.3% | 52.1% | 48.4% | 51.0% |
| PZnE | 1.12349 | 0.07736 | 35.6% | 63.7% | 46.4% | 53.0% |
| PZnEE | 0.97615 | 0.11051 | 30.3% | 68.9% | 47.1% | 52.3% |
| PZnEEE | 1.41511 | 0.18479 | 26.7% | 72.1% | 50.1% | 49.1% |
| EPZnE | 1.25549 | 0.1409 | 26.6% | 73.0% | 48.7% | 50.9% |
| EEPZnEE | 1.11735 | 0.16668 | 18.2% | 81.6% | 45.4% | 54.1% |
| EEEPZnEEE | 1.52562 | 0.33766 | 13.9% | 85.8% | 53.4% | 46.1% |
| PZn-cross | 1.37213 | 0.1234 | -- [c] | -- [c] | -- [c] | -- [c] |

*a* taken as the range from 375nm to 500nm
*b* taken as the range from 500nm to 725nm
*c* due to the $D_{4h}$ symmetry of this molecule, distinct x- and y-polarized transitions are not obtained. Instead two energetically identical transitions of mixed character are calculated (see Fig. S7).

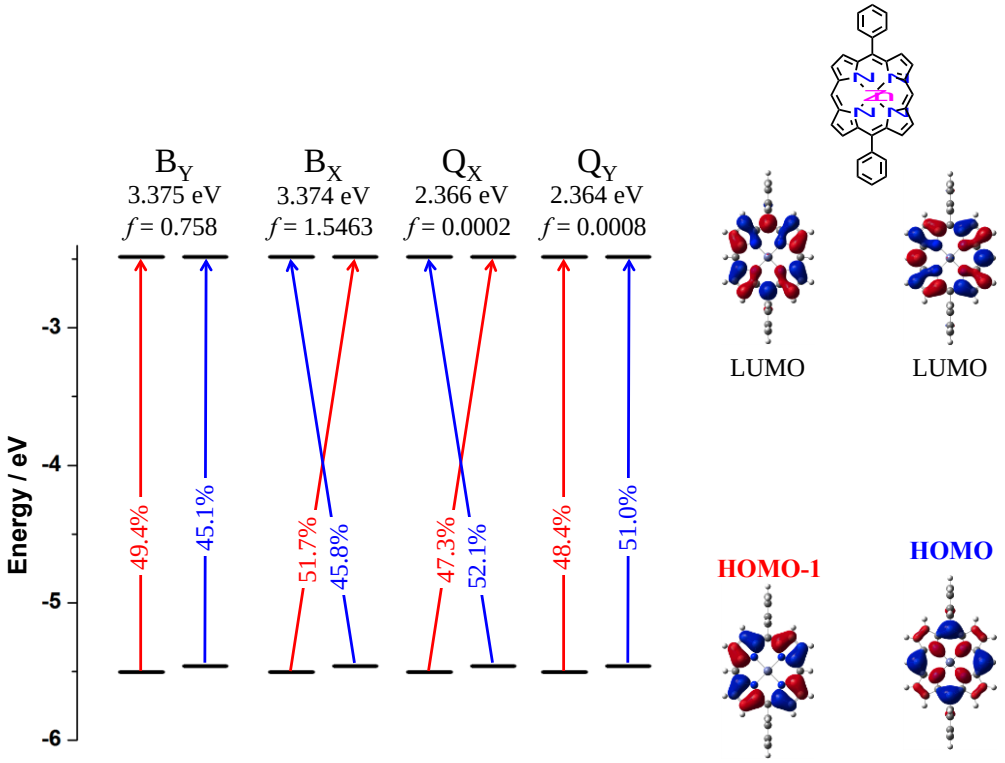


**Fig. S6** TDDFT-calculated major transitions for ZnDPP. Configurations originating from HOMO-1 are represented by red arrows, and those from the HOMO are blue. The percentage of each configuration's contribution to the total transition is noted on the arrows.

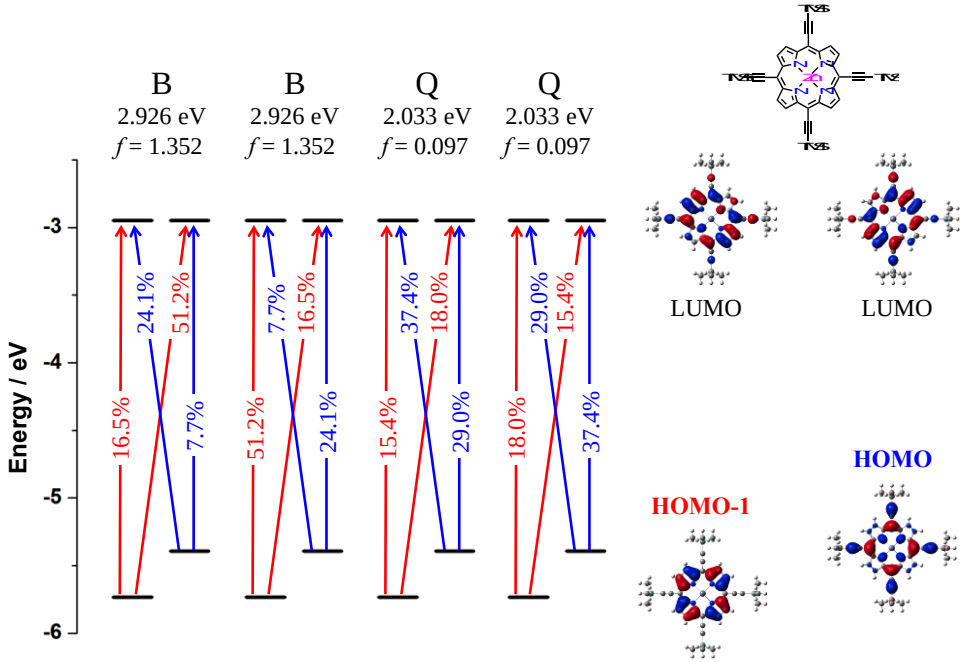


**Fig. S7** TDDFT-calculated major transitions for PZn-cross. Configurations originating from HOMO-1 are represented by red arrows, and those from the HOMO are blue. The percentage of each configuration's contribution to the total transition is noted on the arrows.

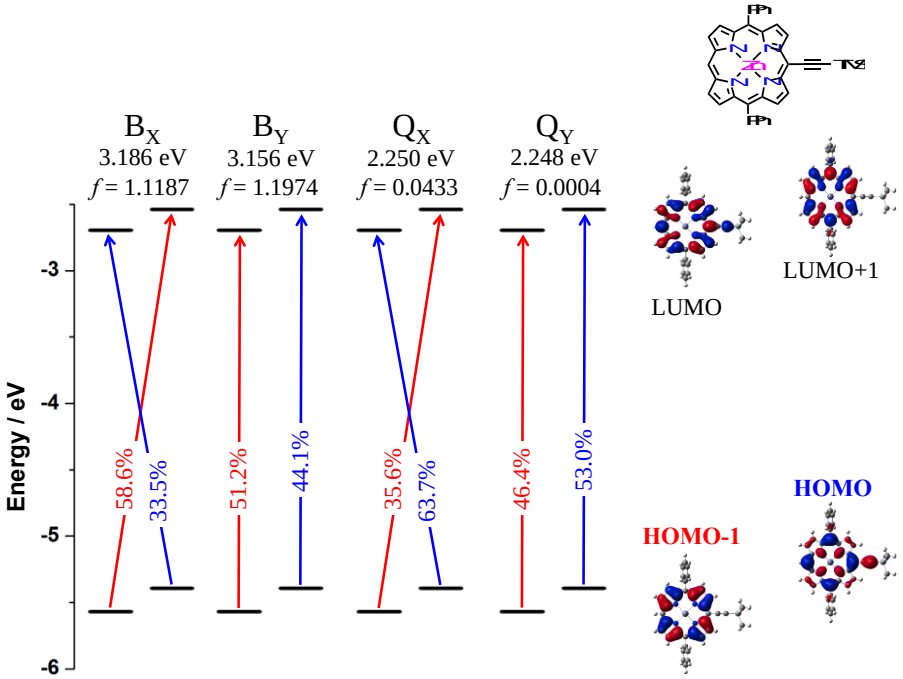


**Fig. S8** TDDFT-calculated major transitions for PZnE. Configurations originating from HOMO-1 are represented by red arrows, and those from the HOMO are blue. The percentage of each configuration's contribution to the total transition is noted on the arrows.

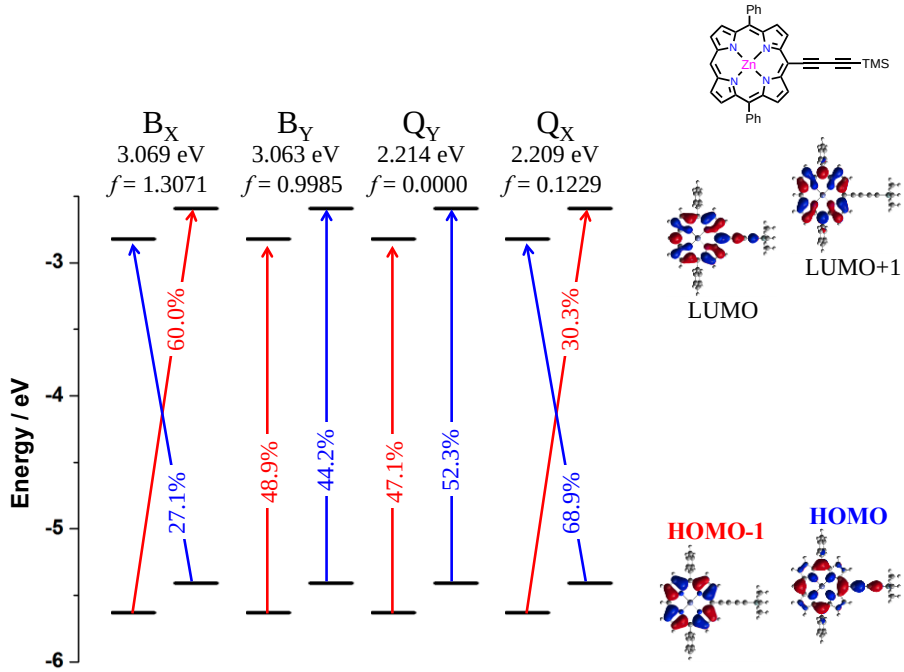


**Fig. S9** TDDFT-calculated major transitions for PZnEE. Configurations originating from HOMO-1 are represented by red arrows, and those from the HOMO are blue. The percentage of each configuration's contribution to the total transition is noted on the arrows.

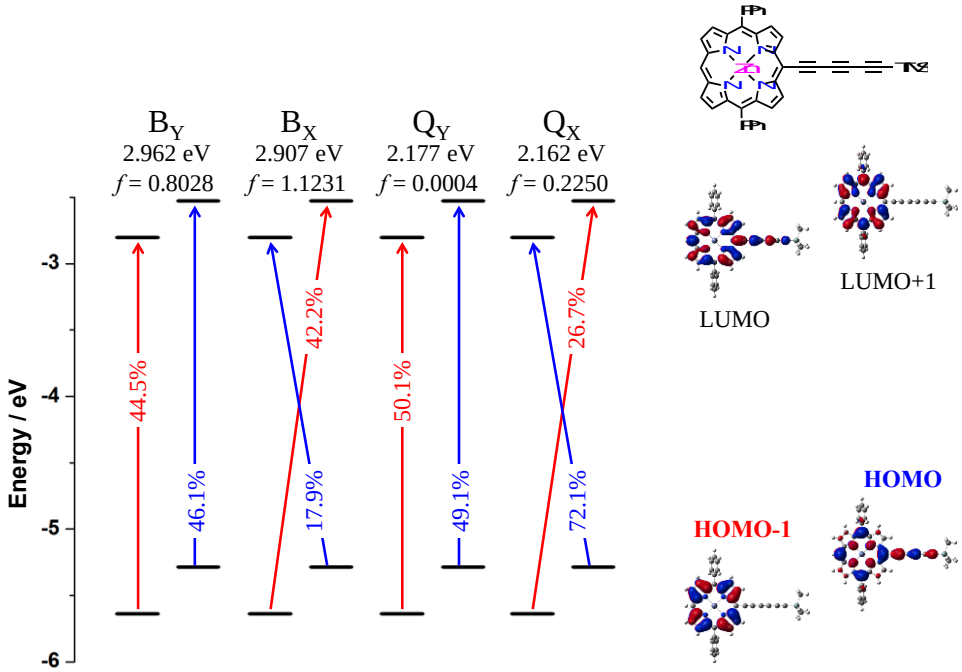


**Fig. S10** TDDFT-calculated major transitions for PZnEEE. Configurations originating from HOMO-1 are represented by red arrows, and those from the HOMO are blue. The percentage of each configuration's contribution to the total transition is noted on the arrows.

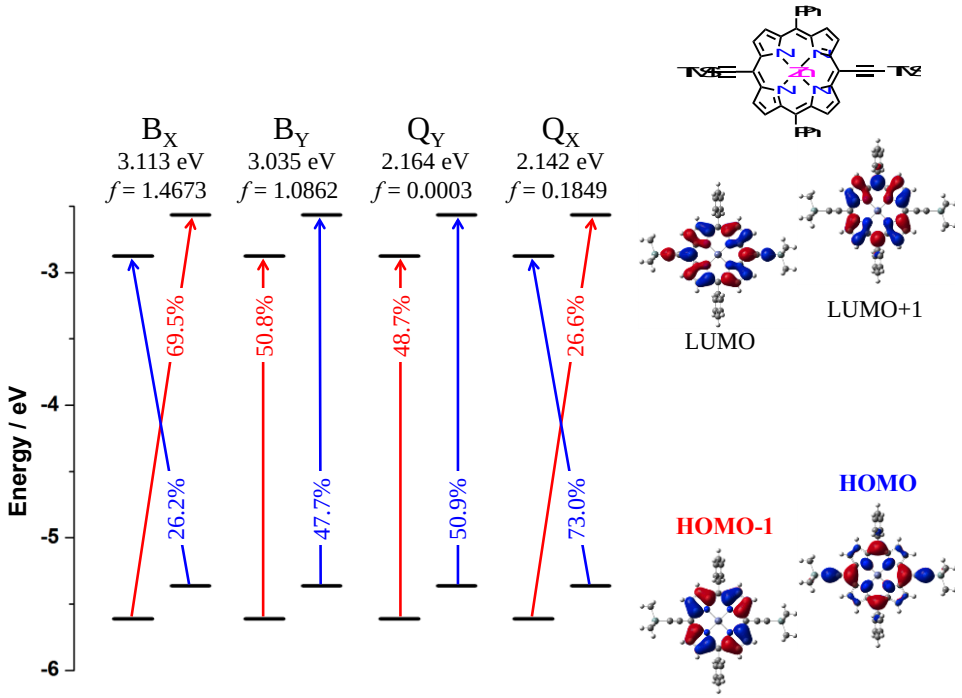


**Fig. S11** TDDFT-calculated major transitions for EPZnE. Configurations originating from HOMO-1 are represented by red arrows, and those from the HOMO are blue. The percentage of each configuration's contribution to the total transition is noted on the arrows.

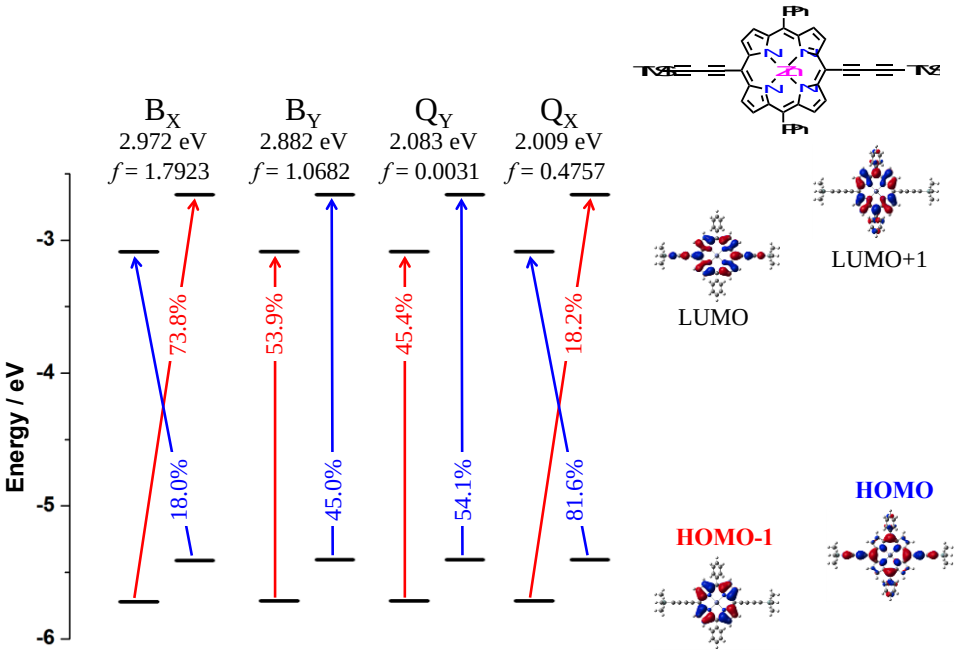


**Fig. S12** TDDFT-calculated major transitions for EEPZnEE. Configurations originating from HOMO-1 are represented by red arrows, and those from the HOMO are blue. The percentage of each configuration's contribution to the total transition is noted on the arrows.

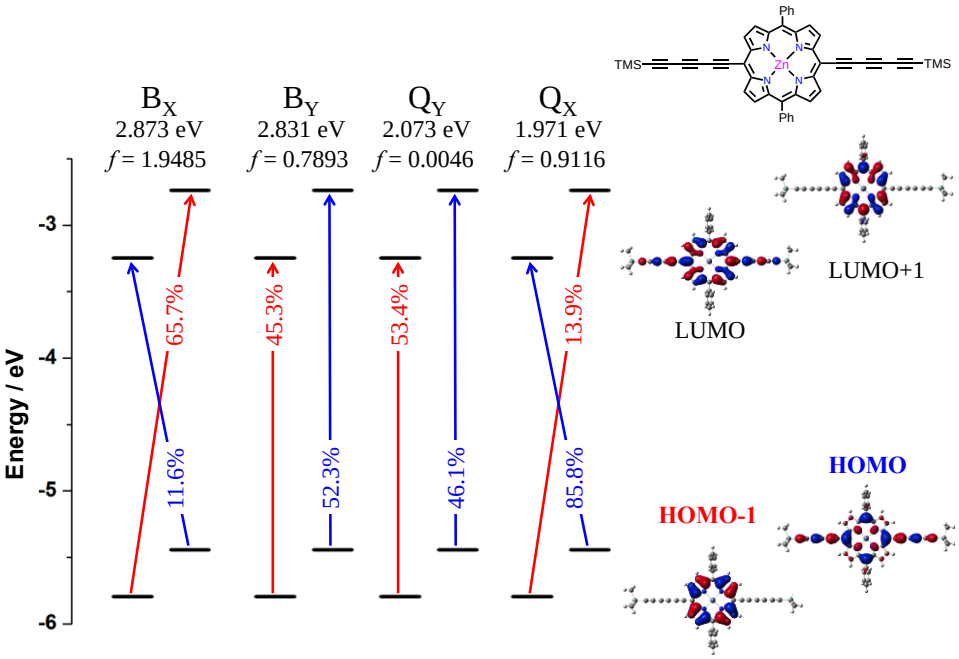


**Fig. S13** TDDFT-calculated major transitions for EEEPZnEEE. Configurations originating from HOMO-1 are represented by red arrows, and those from the HOMO are blue. The percentage of each configuration's contribution to the total transition is noted on the arrows.

## References

1. I. Wavefunction, Irvine, CA, Editon edn., 2010.
2. M. J. Frisch, G. W. Trucks, H. B. Schlegel, G. E. Scuseria, M. A. Robb, J. R. Cheeseman, G. Scalmani, V. Barone, B. Mennucci, G. A. Petersson, H. Nakatsuji, M. Caricato, X. Li, H. P. Hratchian, A. F. Izmaylov, J. Bloino, G. Zheng, J. L. Sonnenberg, M. Hada, M. Ehara, K. Toyota, R. Fukuda, J. Hasegawa, M. Ishida, T. Nakajima, Y. Honda, O. Kitao, H. Nakai, T. Vreven, J. A. Montgomery, J. E. Peralta, F. Ogliaro, M. Bearpark, J. J. Heyd, E. Brothers, K. N. Kudin, V. N. Staroverov, R. Kobayashi, J. Normand, K. Raghavachari, A. Rendell, J. C. Burant, S. S. Iyengar, J. Tomasi, M. Cossi, N. Rega, J. M. Millam, M. Klene, J. E. Knox, J. B. Cross, V. Bakken, C. Adamo, J. Jaramillo, R. Gomperts, R. E. Stratmann, O. Yazyev, A. J. Austin, R. Cammi, C. Pomelli, J. W. Ochterski, R. L. Martin, K. Morokuma, V. G. Zakrzewski, G. A. Voth, P. Salvador, J. J. Dannenberg, S. Dapprich, A. D. Daniels, Farkas, J. B. Foresman, J. V. Ortiz, J. Cioslowski and D. J. Fox, Wallingford CT, Editon edn., 2009.
3. A. D. Becke, *The Journal of Chemical Physics*, 1993, **98**, 5648-5652.
4. (a) C. Lee, W. Yang and R. G. Parr, *Physical Review B*, 1988, **37**, 785-789; (b) B. Miehlich, A. Savin, H. Stoll and H. Preuss, *Chem. Phys. Lett.*, 1989, **157**, 200-206.
5. (a) R. C. Binning and L. A. Curtiss, *J. Comput. Chem.*, 1990, **11**, 1206-1216; (b) J.-P. Blaudeau, M. P. McGrath, L. A. Curtiss and L. Radom, *The Journal of Chemical Physics*, 1997, **107**, 5016-5021; (c) L. A. Curtiss, M. P. McGrath, J.-P. Blaudeau, N. E. Davis, J. R. C. Binning and L. Radom, *The Journal of Chemical Physics*, 1995, **103**, 6104-6113; (d) P. J. Hay, *The Journal of Chemical Physics*, 1977, **66**, 4377-4384; (e) R. Krishnan, J. S. Binkley, R. Seeger and J. A. Pople, *The Journal of Chemical Physics*, 1980, **72**, 650-654; (f) M. P. McGrath and L. Radom, *The Journal of Chemical Physics*, 1991, **94**, 511-516; (g) A. D. McLean and G. S. Chandler, *The Journal of Chemical Physics*, 1980, **72**, 5639-5648; (h) K. Raghavachari and G. W. Trucks, *The Journal of Chemical Physics*, 1989, **91**, 1062-1065; (i) A. J. H. Wachters, *The Journal of Chemical Physics*, 1970, **52**, 1033-1036.
6. M. Gouterman, *J. Mol. Spectrosc.*, 1961, **6**, 138-163.
7. J. K. Laha, S. Dhanalekshmi, M. Taniguchi, A. Ambroise and J. S. Lindsey, *Organic Process Research & Development*, 2003, **7**, 799-812.
8. R. Eastmond and D. R. M. Walton, *Tetrahedron*, 1972, **28**, 4591-4599.
9. M. J. Plater, S. Aiken and G. Bourhill, *Tetrahedron*, 2002, **58**, 2415-2422.
10. H. T. Uyeda, Y. Zhao, K. Wostyn, I. Asselberghs, K. Clays, A. Persoons and M. J. Therien, *J. Am. Chem. Soc.*, 2002, **124**, 13806-13813.
11. I. Y. Chan, W. G. van Dorp, T. J. Schaafsma and J. H. van der Waals, *Mol. Phys.*, 1971, **22**, 741-751.
12. P. J. Angiolillo, V. S.-Y. Lin, J. M. Vanderkooi and M. J. Therien, *J. Am. Chem. Soc.*, 1995, **117**, 12514-12527.